Journal of Southeast University (English Edition) Vol. 28, No. 1, pp. 85 - 93 Mar. 2012 ISSN 1003—7985

Characterizing uncertainty in pavement performance prediction

Sun Lu[1,2] Ge Minli[1] Gu Wenjun[1] Xu Bing[1]

([1]School of Transportation, Southeast University, Nanjing 210096, China)

([2]Department of Civil Engineering, Catholic University of America, Washington DC 20064, USA)

Abstract: Taking variability and uncertainty involved in performance prediction into account, in order to make the prediction reliable and meaningful, a distribution-based method is developed to predict future PSI. This method, which is based on the AASHTO pavement performance model, treats predictor variables as random variables with certain probability distributions and obtains the distribution of future PSI through the method of Monte-Carlo simulation. A computer program PERFORM using Monte Carlo simulation is developed to implement the numerical computation. Simulation results based on pavement and traffic parameters show that traffic, surface layer material property, and initial pavement performance are the most significant factors affecting pavement performance. Once the distribution of future PSI is determined, statistics such as the mean and the variance of future PSI are readily available.

Key words: pavement performance; variability; prediction; Monte Carlo simulation

doi: 10.3969/j.issn.1003 - 7985.2012.01.015

Since the late 1990s, the key role of state transportation agencies has been shifted from the construction of new transportation facilities to the operations and management of existing transportation infrastructure systems[1-4]. Recent National Highway User Surveys conducted by the National Quality Initiative Steering Committee indicated that the public rate pavement smoothness is the most important factor of user satisfaction on highway transportation system performance[4-5].

The present serviceability index (PSI), a 0-5 scale indicator originally developed by Carey and Irick during AASHO road test[6] has been widely used for years as a highway smoothness measure in pavement design and management[1,7-10]. Performance modeling and prediction in terms of smoothness has become a crucial subject in transportation asset management because smoothness is not only the number one factor affecting public rating, but also the primary contributing factor to a number of problems[11]. For instance, rougher pavement surfaces can increase vehicle operation costs due to more fuel consumption and mechanical damage, and can increase pavement damage due to dynamic loads[12].

Tremendous efforts have been made for pavement performance modeling and prediction under uncertainty[1,8-10,13-20]. The most widely used method is statistical regression analysis. Typically one first collects enough pavement related data (e.g., traffic, pavement structural information, material properties, environmental effects, and climate conditions) from a municipal or state pavement system. Statistical regression analysis is performed which relates pavement performance to a number of predictor variables. The developed regression model can then be used for performance prediction. Many performance models have been developed over the years. Most performance models suffer the limitation of being only applicable to local conditions because these models are developed based on locally collected data.

A good exception to the performance model is the pavement design equation specified in the American Association of State Highway and Transportation Officials Pavement Design Guide[7]. Using the same technique (statistical regression), pavement design equation was developed using AASHO road test data, which has high data quality and integrity. More importantly, AASHTO (1993) pavement design equation has been used for pavement design by many states and countries all over the world. Its reliability has been examined in practice for decades.

The AASHTO (1993) pavement design equation is used as a basis for pavement performance modeling and prediction in this paper. A challenge in pavement performance prediction is to characterize variability and uncertainty associated with pavement performance. Because a great amount of variability and uncertainty are involved in performance prediction, it is very important that variability and uncertainty receive necessary treatment so as to make the prediction reliable and meaningful. In this study, we develop a distribution-based method for PSI modeling and prediction using Monte Carlo simulation.

Received 2011-09-14.

Biography: Sun Lu (1972—), male, doctor, professor, sunl@cua.edu.

Foundation items: The US National Science Foundation (No. CMMI-0408390, CMMI-0644552), the American Chemical Society Petroleum Research Foundation (No. PRF-44468-G9), Chang Jiang Scholars Program, the Fok Ying-Tong Education Foundation (No. 114024), the Natural Science Foundation of Jiangsu Province (No. SBK200910046), the Postdoctoral Science Foundation of Jiangsu Province (No. 0901005C).

Citation: Sun Lu, Ge Minli, Gu Wenjun, et al. Characterizing uncertainty in pavement performance prediction[J]. Journal of Southeast University (English Edition), 2012, 28(1): 85 - 93. [doi: 10.3969/j.issn.1003 - 7985.2012.01.015]

1 Pavement Performance Prediction Model

According to AASHTO (1993), the flexible pavement design equation is

$$\log N_{18}(t) = 9.36\log(N_S + 1) - 8.27 + 2.32\log M_R + \left[0.40 + \frac{1\,094}{(N_S + 1)^{5.19}}\right]^{-1} \log\frac{\mathrm{PSI}_0 - \mathrm{PSI}_t}{4.2 - 1.5} \quad (1)$$

$$N_S = a_1 D_1 + a_2 D_2 m_2 + a_3 D_3 m_3 \quad (2)$$

where $N_{18}(t)$ is the cumulative number of equivalent single axle load (ESAL); M_R is the effective roadbed soil resilient modulus; PSI_0 is the initial PSI, and PSI_t is the PSI at time t after carrying $N_{18}(t)$ cumulative ESAL; m_2 and m_3 are drainage coefficients for base and subbase layers, respectively; $a_i (i = 1, 2, 3)$ are the layer coefficients representative of surface, base, and subbase courses, respectively; and $D_i (i = 1, 2, 3)$ is the actual (in inches) thickness of each layer; N_S is the pavement structure number, which reflects the structural capacity to carry traffic loads and can be calculated from Eq. (2) in terms of pavement thickness and material property[7, 9, 21].

Eq. (1) is established based on the AASHO road test data for highway pavement design purposes[8]. It is essentially an empirical model developed using statistical regression analysis. According to the regression theory, the dependent variable (the left-hand side of Eq. (1)) is the mean cumulative ESAL. If Eq. (1) is to be used for predicting the cumulative ESAL, a normally distributed additive error term $\varepsilon \sim N(0, \sigma_\varepsilon^2)$ should be added to the right-hand side of Eq. (1)[22-23]. After mathematical manipulation, pavement performance PSI at time t can be expressed as a function of predictor variables,

$$\mathrm{PSI}_t = \mathrm{PSI}_0 - 2.7\left[\frac{N_{18}(t)\,10^{8.27-\varepsilon}}{M_R^{2.32}(N_S + 1)^{9.36}}\right]^{(0.4 + 1\,094/(N_S+1)^{5.19})} \quad (3)$$

where $\varepsilon \sim N(0, 0.35^2)$ can be found from AASHTO (1993). The interpretation of Eq. (3) is that if the values of predictor variables PSI_0, M_R, N_S and $N_{18}(t)$ are available, PSI at time t can be predicted accordingly.

2 Uncertainty in Performance Modeling and Prediction

If each predictor variable in the right-hand side of Eq. (3) is deterministic and known with certainty, the prediction of PSI_t becomes a matter of straightforward substitution and computation using Eq. (3). In reality, however, a great deal of uncertainty is involved in pavement performance modeling and prediction. Basically, there are six different sources of uncertainty:

1) Missing or nonobservable contributing factors. Pavement performance model (3) is derived from regression model (1). It is not uncommon in regression analysis that only part of the predictor (explanatory) variables are included in the regression model. In other words, pavement performance may also be affected by other factors, of which the modeler is not fully aware, and therefore these contributing factors are not included in the performance model.

2) Functional misspecification. The performance model is only a data-driven empirical model. The function form in (1) is not known with certainty. The modeler must assume a functional relationship, for instance, a linear relationship.

3) Variability associated with the pavement material and the structural properties. Pavement material and structural properties are rarely deterministic constants as designed. Due to the very nature of highway spatial distribution, there is always variability associated with thickness, modulus, and other variables as reflected in the right-hand side of Eq. (3).

4) Finite sampling. Because samples can be taken from only a finite number of locations along a highway with regard to the measurement of the pavement material and the structural properties, such finite samples may not well represent the pavement material and the structural properties of the whole highway system.

5) Measurement error. There are always measurement errors embedded in the measurement of each of the predictor variables. The magnitude and distribution of the measurement error depend upon the equipment accuracy.

6) Unforeseen future. According to Eq. (3), cumulative traffic is a contributing factor affecting future pavement performance. To predict pavement performance using Eq. (3), future traffic must be provided as a known factor, which itself, however, has to be forecasted first. Due to the inability to foresee the future, it is impossible to precisely forecast future traffic.

Among these sources of uncertainty, 1) and 2) are related to function fitting. Although uncertainty will never be eliminated, it can be reduced if careful statistical analysis and data mining techniques are applied. Good construction quality control can reduce the uncertainty introduced in 3) to some degree, but will never eliminate it. Increasing sampling frequency can reduce the uncertainty in 4), while more accurate measuring devices can reduce the uncertainty in 5). For the uncertainty in 6), long-term recording of traffic history can help to make more reliable traffic forecasts.

To predict future PSI_t, it is of paramount importance that uncertainty resulting from various sources is taken into account properly. We propose a distribution-based method to fulfill the task of performance prediction. The basic idea of this method is to treat all independent variables in Eq. (3) as random variables, and to predict the

distribution of dependent variable PSI_t. In this paper, it is assumed that the measurement of predictor variables is accurate, i. e., no uncertainty concerning measurement. Uncertainty except in 2) in the list is considered here. The error term ε in Eq. (3) accounts for the model uncertainty. Since the pavement material and the structural properties are treated as random variables, their distributions need to be estimated from field samples. Similarly, cumulative traffic at future time t is also treated as a random variable with a certain distribution, which, clearly, is a function of time.

3 Distribution-Based Sensitivity Analysis Using Simulation

In traditional sensitivity analysis one variable at a time is allowed to vary within a specified range[24]. It is the bounds of the range rather than the distribution of the changeable variables within the range that are important. We develop a distribution-based sensitivity analysis in this study. Similar to traditional sensitivity analysis, only one factor at a time is allowed to vary and all other remaining factors stay unchanged; however, instead of specifying bounds for each random variable, probability distributions and associated parameters are specified. In other words, for each predictor variable, a specified number of random values are first generated in accordance with the pre-defined distribution. These random values are then substituted into performance prediction equation (3) to calculate future performance. Distribution-based sensitivity analysis allows one to observe the variation of predicted performance at time t with respect to a single variable, and therefore help the understanding of the influence of different contributing factors to future pavement performance.

Under this framework of the distribution-based method, the problem of performance prediction becomes an estimation of the probability distribution of PSI_t as a function of random variables. In theory, the expression of the distribution of PSI_t can be obtained analytically, but the implementation is cumbersome because it requires numerical evaluation of multidimensional integration. Monte Carlo simulation is utilized in this study for the implementation of performance prediction. The key steps involved in implementation performance prediction using Monte Carlo simulation include 1) random number generation, 2) random variable generation, 3) computing the predicted performance using Eq. (3), and 4) statistical analyses of simulated performance.

The basic ingredient needed for every method of generating random variables from any probability distribution or stochastic process is a source of identically and independently distributed (iid) uniform $U(0,1)$ random variables. For this reason, it is essential that a statistically reliable $U(0,1)$ random number generator be available. In this study, a linear congruential generator (LCG) introduced by Ref. [25] is used for this purpose. A sequence of integers $Z_1, Z_2, \cdots$ is defined by the recursive formula

$$Z_i = (aZ_{i-1} + c) \bmod m \tag{4}$$

where m is the modulus; a is the multiplier; c is the increment; and Z_0 is the seed. They are all nonnegative integers. According to Eq. (4), it is clear that $0 \leqslant Z_i \leqslant m-1$ and the desired uniformly distributed random number $U_i = Z_i/m$. In order to maintain that the generated random number possesses good statistical properties, care must be taken for choosing the appropriate parameters. In this paper, we use $m = 2^{31} - 1$, $a = 630\,360\,016$, and $c = 0$.

There are many techniques for generating random variables (e. g., inverse transform, convolution, composition, acceptance-rejection), and the particular algorithm used should depend on the distribution from which we wish to generate. In this paper, two types of continuous distribution are used: uniform distribution and normal distribution. Therefore, only algorithms related to generating these two types of random variables are presented. Random variables following other types of distribution can also be obtained using simulation. They will not be all listed here and one may refer to Law and Kelton[26] for details.

The distribution function of a $U(a,b)$ random variable is easily obtained by inverting $u = F(x)$,

$$x = F^{-1}(u) = a + (b-a)u \qquad 0 \leqslant u \leqslant 1 \tag{5}$$

The inverse transform method can thus be used to generate X: 1) generate $U \sim U(0,1)$, and 2) return $X = a + (b-a)U$. The constant $b-a$ should be computed beforehand and stored for use in the algorithm to save the computational effort. To generate normally distributed random variables, the polar method[27] is used and it follows that:

1) Generate U_1 and U_2 as iid $U(0,1)$; 2) Let $V_i = 2U_i - 1$ for $i = 1,2$; 3) $W = V_1^2 + V_2^2$. If $W > 1$, go back to step 1). Otherwise, let $Y = \sqrt{(-2\ln W)/W}$, $X_1 = V_1 Y$ and $X_2 = V_2 Y$. Then X_1 and X_2 are iid $N(0,1)$ random variables. In step 2) a "rejection" of U_1 and U_2 can occur with probability $1 - \pi/4$.

A computer program called PERFORM has been developed using Visual Basic based on the methods outlined so far. The input of PERFORM is the probability distribution and associated parameters for each variable in the right-hand side of Eq. (3). The output of PERFORM predicts PSI_t and produces random samples of PSI_t. This information can be used to estimate its probability density function (PDF), cumulative density function (CDF), mean, standard deviation, confidence interval, median, skewness, kurtosis, quintiles, and many other statistics of PSI_t.

4 Numerical Study

4.1 Effect of model error and traffic

The effects of model error, increasing cumulative ESAL and traffic uncertainty on future performance are studied in two scenarios. In scenario 1, all the variables except the model error, which is a normally distributed random variable, are assumed to be constant taken from typical pavement structures as follows: $D_1 = 8$, $D_2 = 7$, $D_3 = 11$, $m_2 = 1.25$, $m_3 = 1.15$, $a_1 = 0.35$, $a_2 = 0.14$, $a_3 = 0.11$, $M_R = 5\,000$, $PSI_0 = 4.5$ and $\varepsilon \sim N(0, 0.35^2)$, while cumulative traffic ESAL is set up at levels $N_{18} = 1 \times 10^5, 2 \times 10^5, \cdots, 10 \times 10^5$. The statistics of the simulation results are shown in Tab. 1. Comparing the mean and the median of the PSI, it is found that the mean is always less than the median, meaning that the PSI is not symmetrically distributed. Further analysis indicates that the skewness of PSI is -0.895.

Tab. 1 PSI vs. traffic N_{18}

ESAL/10^5	1	2	3	4	5	6	7	8	9	10
Mean	4.500	4.371	4.322	4.284	4.253	4.225	4.201	4.178	4.157	4.138
Median	4.500	4.380	4.334	4.299	4.270	4.244	4.221	4.200	4.181	4.163
Std	0.000	0.050	0.070	0.084	0.097	0.107	0.117	0.126	0.134	0.142
CV	0.000	0.012	0.016	0.020	0.023	0.025	0.028	0.030	0.032	0.034

Fig. 1 plots the cumulative density function of PSI vs. traffic. In Fig. 1, curves from bottom up correspond to ESAL = $1 \times 10^5, 2 \times 10^5, \cdots, 10 \times 10^5$ replications, respectively. As can be seen from Tab. 1, the coefficient of variation (CV) increases from 0.012 to 0.034 as cumulative ESAL increases from 1×10^5 to 10×10^5. The spreading of PSI increases when ESAL increases as illustrated in Fig. 1. This indicates that the variability of PSI will increase as ESAL increases, even if there is no variability in the pavement material and structure, and traffic. Such variability in PSI is caused by pavement performance model uncertainty mentioned in the previous section, which propagates and aggrandizes through the pavement performance model.

Variables in scenario 2 are the same as those in scenario 1 except that cumulative traffic ESAL is related to time according to $N_{18}(t) \sim N(800\,000t, (100\,000\sqrt{t})^2)$, in which t is time in years and $N(\,)$ is a normal distribution. The simulation results are shown in Tab. 2 and Fig. 2. In Fig. 2 curves from bottom up correspond to Time = 1, 2, $\cdots$, 10 year, respectively. It can be seen that as time increases, the mean PSI decreases while the variability of PSI in terms of CV increases considerably. Since uncertainty associated with cumulative traffic ESAL is involved in this scenario, the interaction between traffic and model uncertainty results in further spreading of PSI as time progresses.

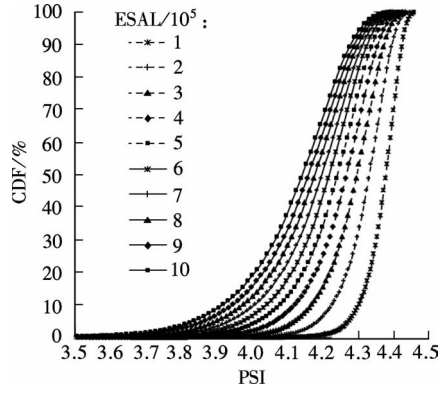

Fig. 1 Cumulative density function of PSI vs. ESAL

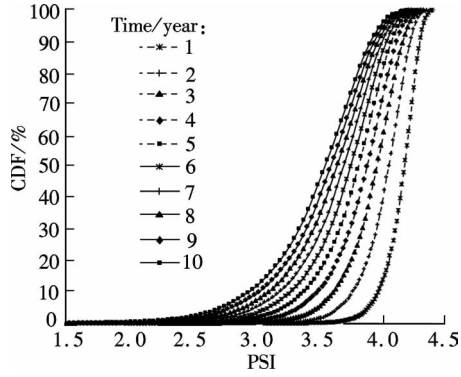

Fig. 2 Cumulative density function of PSI vs. time

Tab. 2 PSI vs. time t

Time/year	1	2	3	4	5	6	7	8	9	10
Mean	4.500	4.180	4.055	3.962	3.884	3.815	3.752	3.696	3.644	3.595
Median	4.500	4.155	4.022	3.921	3.837	3.764	3.697	3.637	3.581	3.528
Std	0.000	0.138	0.190	0.229	0.262	0.290	0.317	0.340	0.363	0.383
CV	0.000	0.033	0.047	0.058	0.068	0.077	0.086	0.094	0.101	0.109

4.2 Effect of layer thickness

Three scenarios are examined to study the effect of different pavement layer thicknesses D_1, D_2, D_3 on future performance. In Tab. 3, $N(\mu, \sigma^2)$ stands for a normal distribution with mean μ and standard deviation σ. All the other variables besides the layer thickness are identical to that described in scenario 1 in section

4.1. The CV of PSI is shown in Fig. 3, in which different curves from bottom up correspond to ESAL = $1\times10^5, 2\times10^5, \cdots, 10\times10^5$ replications, respectively. The CV of PSI at various levels of traffic and thickness variations increases linearly with the increase in the standard deviation of layer thickness. However, for the pavement structure simulated in this paper, the range of CV of PSI is within 5% of the mean value of PSI.

Tab. 3 Three scenarios of various distributions of layer thickness

Scenario 1	Scenario 2	Scenario 3
$D_1 = 8$	$D_2 = 7$	$D_3 = 11$
$D_1 \sim N(8, 0.1^2)$	$D_2 \sim N(7, 0.1^2)$	$D_3 \sim N(11, 0.2^2)$
$D_1 \sim N(8, 0.2^2)$	$D_2 \sim N(7, 0.2^2)$	$D_3 \sim N(11, 0.4^2)$
$D_1 \sim N(8, 0.3^2)$	$D_2 \sim N(7, 0.3^2)$	$D_3 \sim N(11, 0.6^2)$
$D_1 \sim N(8, 0.4^2)$	$D_2 \sim N(7, 0.4^2)$	$D_3 \sim N(11, 0.8^2)$
$D_1 \sim N(8, 0.5^2)$	$D_2 \sim N(7, 0.5^2)$	$D_3 \sim N(11, 1.0^2)$
$D_1 \sim N(8, 0.6^2)$	$D_2 \sim N(7, 0.6^2)$	$D_3 \sim N(11, 1.2^2)$
$D_1 \sim N(8, 0.7^2)$	$D_2 \sim N(7, 0.7^2)$	$D_3 \sim N(11, 1.4^2)$
$D_1 \sim N(8, 0.8^2)$	$D_2 \sim N(7, 0.8^2)$	$D_3 \sim N(11, 1.6^2)$
$D_1 \sim N(8, 0.9^2)$	$D_2 \sim N(7, 0.9^2)$	$D_3 \sim N(11, 1.8^2)$
$D_1 \sim N(8, 1.0^2)$	$D_2 \sim N(7, 1.0^2)$	$D_3 \sim N(11, 2.0^2)$
$D_1 \sim N(8, 1.1^2)$	$D_2 \sim N(7, 1.1^2)$	
$D_1 \sim N(8, 1.2^2)$	$D_2 \sim N(7, 1.2^2)$	

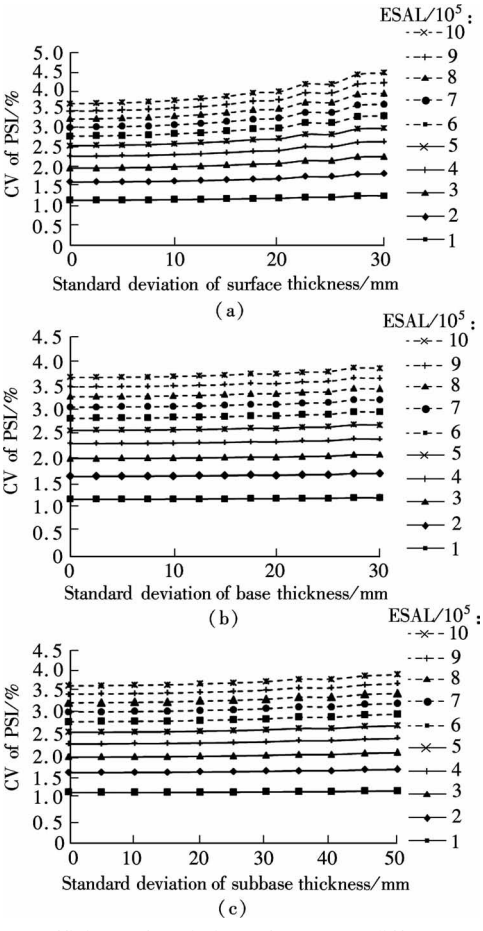

Fig. 3 Coefficient of variation of PSI vs. different pavement layer thicknesses D_1, D_2, D_3. (a) CV of PSI vs. surface thickness; (b) CV of PSI vs. base thickness; (c) CV of PSI vs. subbase thickness

4.3 Effect of material properties

Three scenarios as shown in Tab. 4 are created to study the effects of different pavement layer material properties a_1, a_2, a_3 on future performance. Similarly, all the other variables are identical to those in scenario 1 in section 4.1. The results are plotted in Fig. 4. At light traffic accu mulation, the CV of PSI increases linearly with the incr ease in the standard deviation of layer properties, while this relationship becomes nonlinear as traffic becomes heavier. The range of CV of PSI is within about 10% of the mean PSI.

Tab. 4 Three scenarios of various distributions of material properties

Scenario 1	Scenario 2	Scenario 3
$a_1 = 0.35$	$a_2 = 0.14$	$a_3 = 0.11$
$a_1 \sim N(0.35, 0.02^2)$	$a_2 \sim N(0.14, 0.01^2)$	$a_3 \sim N(0.11, 0.008^2)$
$a_1 \sim N(0.35, 0.04^2)$	$a_2 \sim N(0.14, 0.02^2)$	$a_3 \sim N(0.11, 0.016^2)$
$a_1 \sim N(0.35, 0.06^2)$	$a_2 \sim N(0.14, 0.03^2)$	$a_3 \sim N(0.11, 0.024^2)$
$a_1 \sim N(0.35, 0.08^2)$	$a_2 \sim N(0.14, 0.04^2)$	$a_3 \sim N(0.11, 0.032^2)$
$a_1 \sim N(0.35, 0.10^2)$	$a_2 \sim N(0.14, 0.05^2)$	$a_3 \sim N(0.11, 0.040^2)$

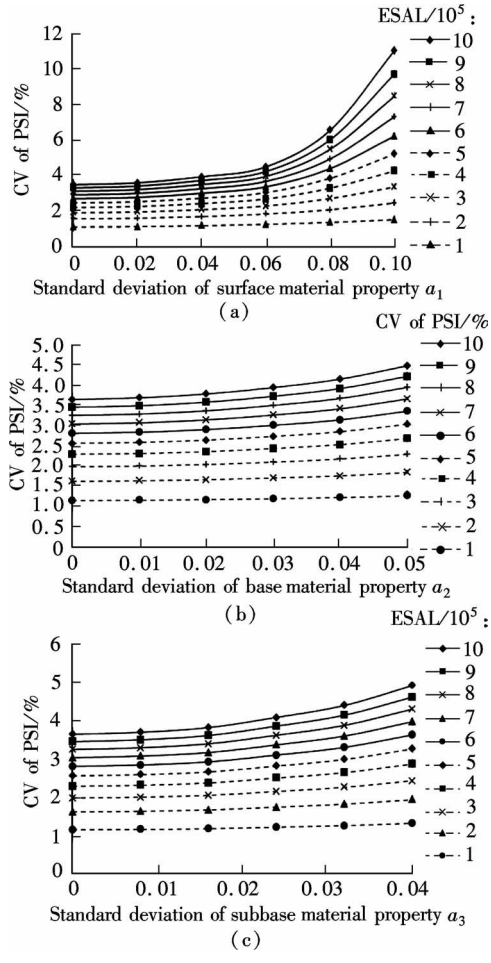

Fig. 4 Coefficient of variation of PSI vs. different layer material properties a_1, a_2, a_3. (a) CV of PSI vs. surface material a_1; (b) CV of PSI vs. base material a_2; (c) CV of PSI vs. subbase material a_3

4.4 Effect of drainage conditions

The effects of different pavement layer drainage conditions m_2, m_3 on future performance are investigated. Three scenarios are shown in Tab. 5, where $U(a, b)$ stands for uniform distribution, and a and b are lower and upper bounds. Once again, all the other variables are identical to those in scenario 1 in section 4.1. The results are provided in Fig. 5.

Tab. 5 Scenarios corresponding to base and subbase layer drainage coefficients

U	(1) $U(1.30,1.35)$	(2) $U(1.15,1.25)$	(3) $U(1.05,1.15)$	(4) $U(0.80,1.05)$	(5) $U(0.75,0.95)$
(1) $U(1.30,1.35)$	$m_2=(1), m_3=(1)$	$m_2=(1), m_3=(2)$			
(2) $U(1.15,1.25)$	$m_2=(2), m_3=(1)$	$m_2=(2), m_3=(2)$	$m_2=(2), m_3=(3)$		
(3) $U(1.05,1.15)$		$m_2=(3), m_3=(2)$	$m_2=(3), m_3=(3)$	$m_2=(3), m_3=(4)$	
(4) $U(0.80,1.05)$			$m_2=(4), m_3=(3)$	$m_2=(4), m_3=(4)$	$m_2=(4), m_3=(5)$
(5) $U(0.75,0.95)$				$m_2=(5), m_3=(4)$	$m_2=(5), m_3=(5)$

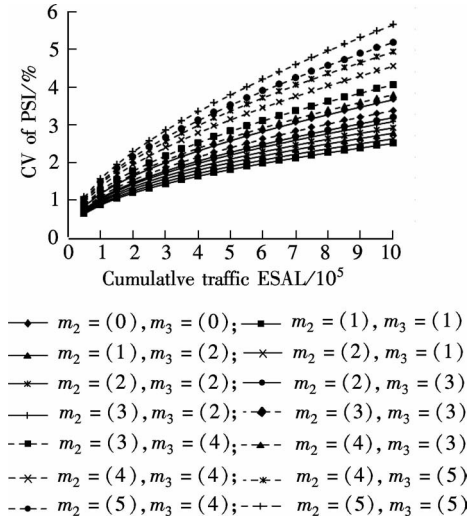

Fig. 5 Coefficient of variation of PSI vs. drainage coefficients m_2 and m_3

4.5 Effect of soil resilient modulus

The effect of soil resilient modulus M_R on future performance is investigated with all the other variables identical to those in scenario 1 in section 4.1. The results corresponding to seven normal distribution scenarios $M_R \sim N(5\,000, 100^2)$, $N(5\,000, 200^2)$, $N(5\,000, 300^2)$, $N(5\,000, 400^2)$, $N(5\,000, 500^2)$, $N(5\,000, 600^2)$, and $N(5\,000, 700^2)$ are provided in Fig. 6. The CV of PSI increases linearly with the increase in the standard deviation of the soil resilient modulus. The range of CV of PSI is within about 5% of the mean PSI.

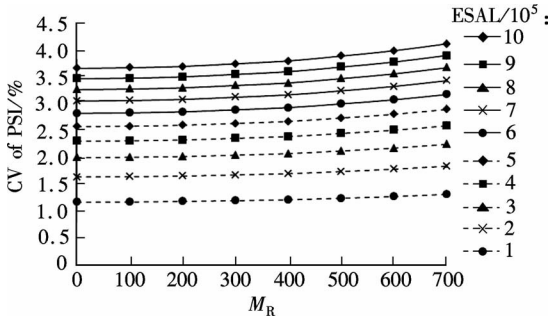

Fig. 6 Coefficient of variation of PSI vs. soil resilient modulus M_R

4.6 Effect of initial performance

According to Eq. (3), future PSI_t is linearly related to initial PSI_0 in such a manner that when uncertainty of PSI_0 propagates through Eq. (3), there is neither amplification nor shrinkage of uncertainty in PSI_0, and there is not interaction between PSI_0 and other predictor variables. The results corresponding to five distribution scenarios $PSI_0 \sim N(4.5, 0.05^2)$, $PSI_0 \sim N(4.5, 0.1^2)$, $PSI_0 \sim N(4.5, 0.15^2)$, $PSI_0 \sim N(4.5, 0.2^2)$, and $PSI_0 \sim N(4.5, 0.25^2)$ are provided in Fig. 7. The CV of PSI increases nonlinearly with the increase in the standard deviation of initial PSI. The range of CV of PSI is within about 10% of the mean PSI.

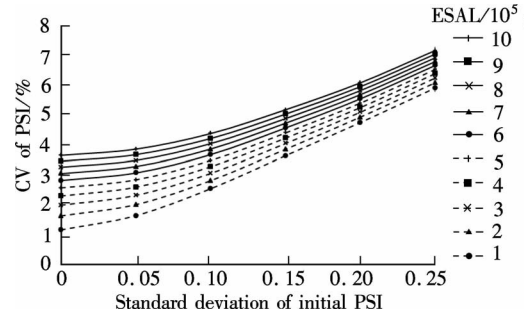

Fig. 7 Coefficient of variation of PSI vs. initial pavement performance PSI_0

5 Uncertainty Propagation Through Performance Model

So far the effect of each single predictor variable on future pavement performance in terms of PSI has been examined in previous sections. In this section complicated but more realistic scenarios are investigated in which all predictor variables are simultaneously treated as random variables with various probability distributions.

First, the effect of the number of simulation runs on the accuracy of performance prediction is investigated. The assumptions are as follows: $D_1 \sim N(8, 1.0^2)$, $D_2 \sim N(7, 1.5^2)$, $D_3 \sim N(11, 2.0^2)$, $a_1 \sim N(0.35, 0.06^2)$, $a_2 \sim N(0.14, 0.04^2)$, $a_3 \sim N(0.11, 0.015^2)$, $m_2 \sim U(1.15, 1.25)$, $m_3 \sim U(1.05, 1.15)$, $M_R \sim N(5\,000, 500^2)$, PSI_0

$\sim N(4.5, 0.1^2)$, $\varepsilon \sim N(0, 0.35^2)$, and cumulative traffic ESAL $N_{18}(t) \sim N(800\,000t, (100\,000\sqrt{t})^2)$, in which t is time in years. These variables are treated as independent random variables. The mean, standard deviation and CV of the predicted PSI_t at the end of the first, fifth and tenth years are plotted in Fig. 8, respectively.

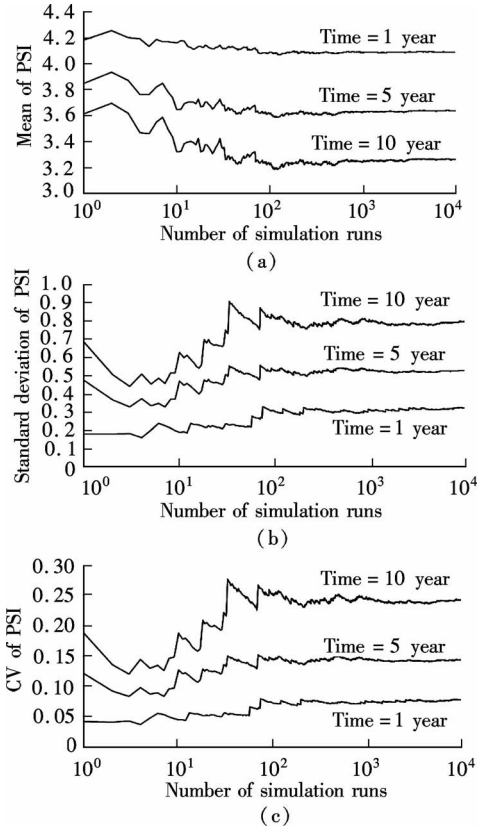

Fig. 8 Mean, standard deviation and coefficient of variation of PSI vs. number of simulation runs. (a) Mean PSI; (b) Standard deviation of PSI; (c) Coefficient of variation of PSI

As can be seen from these figures, there are significant fluctuations in each of these statistics when the number of simulation runs is small, say less than 100. The fluctuation goes through a transition period when the number of simulation runs increases from 100 to 1 000. As the number of simulation runs approaches 10 000, all three statistics asymptotically tend to become stable and remain at a fixed level, which can ensure an accurate simulation result of performance prediction. Based on this analysis, the number of simulation runs is chosen as 10 000 in all the scenarios studied in this paper.

Since all the predictor variables in this scenario are random variables, the prediction of future performance becomes complicated owing to the complex interaction among the predictor variables in Eq. (3). Descriptive statistics of predicted PSI_t are shown in Figs. 9 to 12, respectively. As time increases, both the mean and the median of predicted PSI_t decrease nonlinearly from 4.2 to 3.4, while the standard deviation and CV of predicted PSI_t increase considerably. Fig. 9 shows that the median is always greater than the mean, meaning that the distribution of PSI_t is asymmetric and there is consistent skewness at all time (e.g., for different cumulative ESAL). It is further evident in Fig. 11 that the skewness of predicted PSI_t is always negative, suggesting that the distribution has a long tail towards the left-hand side of the mean. The kurtosis in Fig. 12 decreases from 25 to 2, meaning that as time increases, PSI_t distributes more widely with heavy tails rather than a sharp peak. Figs. 13 and 14 provide a 3-dimensional view of PSI_t vs. time and its PDF and CDF, which further confirms the conclusions.

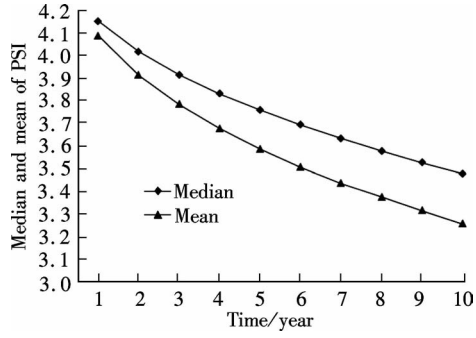

Fig. 9 Mean and median of predicted PSI vs. time

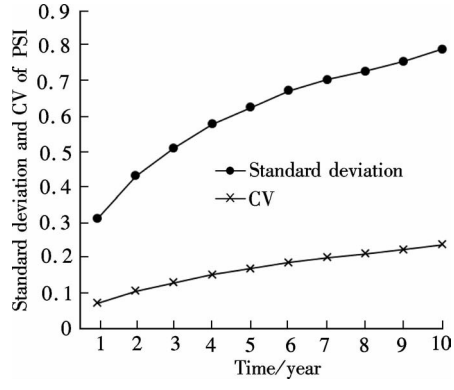

Fig. 10 Coefficient of variation of predicted PSI vs. time

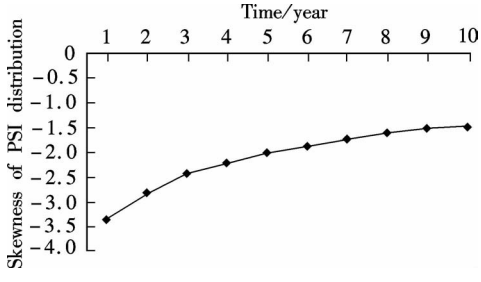

Fig. 11 Skewness of predicted PSI vs. time

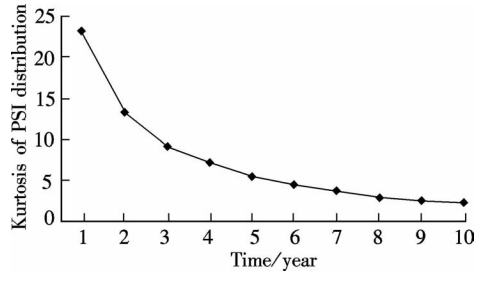

Fig. 12 Kurtosis of predicted PSI vs. time

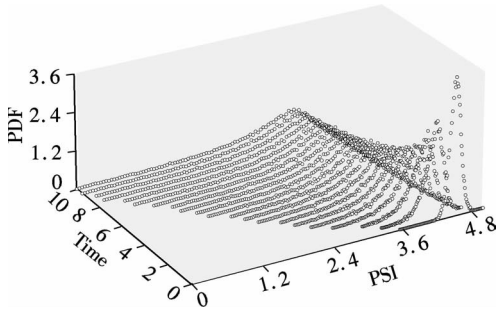

Fig. 13 3-D view of PSI_t vs. time and its probability density function

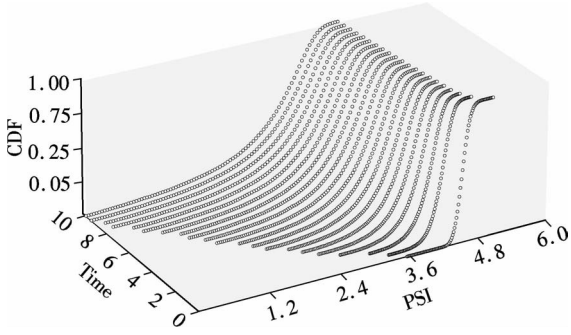

Fig. 14 3-D view of PSI_t vs. time and its cumulative density function

6 Conclusion

In this paper, a pavement performance prediction model is formulated based on the AASHTO pavement design equation. Uncertainty associated with future pavement performance in terms of PSI is affected by the variability of pavement material and structural properties, the uncertainty of performance model, and the uncertainty of predicted cumulative traffic. A distribution-based method is developed to predict future PSI based on the pavement performance model. This method treats all the predictor variables as random variables with certain distributions. A computer program PERFORM using Monte Carlo simulation is developed to implement the numerical computation. Simulation results based on pavement and traffic parameters used in this paper show that traffic, surface layer material property and initial pavement performance are the most significant factors affecting pavement performance. The distribution-based method is more capable than conventional methods to deliver more accurate performance prediction. The methodology, pavement performance model, and computer software PERFORM can be used by transportation agencies for pavement management purposes.

References

[1] Hudson W R, Hass R, Uddin W. *Infrastructure management*[M]. McGraw Hill, 1997.

[2] Irrgang F C, Maze T H. Status of pavement management systems and data analysis models at state highway agencies [J]. *Transportation Research Record*, 1993(1397): 1 - 6.

[3] National Quality Initiative Steering Committee. National highway user survey [R]. Washington DC: National Quality Initiative Steering Committee, 1996.

[4] National Quality Initiative Steering Committee. National highway user survey [R]. Washington DC: National Quality Initiative Steering Committee, 2001.

[5] National Quality Initiative Steering Committee. National highway user survey [R]. Washington DC: National Quality Initiative Steering Committee, 2002.

[6] National Academy of Sciences. The AASHO road test, pavement research, Special Report 61E [R]. Washington DC: Highway Research Board, National Academy of Sciences, 1962.

[7] American Association of State Highway and Transportation Officials. AASHTO guide for design of pavement structures[R]. Washington DC: American Association of State Highway and Transportation Officials, 1993.

[8] Darter M L, Hudson W R. Probabilistic design concepts applied to flexible pavement system design, Report No. 123-18 [R]. Austin, TX, DSA: University of Texas at Austin, 1973.

[9] Haas R, Hudson W R, Zaniewski J P. *Modern pavement management* [M]. Malabar, FL, USA: Krieger Publishing Co., 1994.

[10] Hudson W R. State-of-the-art in predicting pavement reliability from input variability, Report No. FAA-RD-75-207 [R]. Vicksburg: US Army Waterways Experiment Station, 1975.

[11] Cambridge Systematics, Inc. A guidebook for performance-based transportation planning, NCHRP Report 446 [R]. Washington DC: National Academy Press, 2000.

[12] Gillespie T D, Sayers M W, Segel L. Calibration of response-type road roughness measurement systems, NCHRP Report 228 [R]. Washington DC: National Cooperative Highway Research Program, 1980.

[13] *Federal Highway Administration*. VESYS 3A-M user manual [M]. Washington DC: Office of Research and Development, Federal Highway Administration, 1983.

[14] Alsherri A, George K P. Reliability model for pavement performance[J]. *Journal of Transportation Engineering, ASCE*, 1988, **114**(5): 294 - 306.

[15] Jorge K P, Alsherri A, Shah N S. Reliability analysis of premium pavement design features[J]. *Journal of Transportation Engineering, ASCE*, 1988, **114**(3): 278 - 293.

[16] Kenis W. Predicted design procedure for flexible pavement using the VESYS structural subsystem[C]//*Proc Fourth Int Conf Struct Design of Asphalt Pavements*. Ann Arbor, MI, USA: University of Michigan, 1977: 101 - 130.

[17] Kenis W, Wang W. Analysis of pavement structural variability, FHWA-RD-97-072 [R]. Washington DC: Federal Highway Administration, 1997.

[18] Kher R K, Darter M I. Probabilistic concepts and their applications to AASHTO interim guide for design of rigid pavements[J]. *Highway Research Record*, 1973(466): 20 - 36.

[19] Lemer A C, Moavenzadeh F. Reliability of highway

pavements[J]. *Highway Research Record*, 1971(362): 1-8.
[20] Sun L, Hudson W R, Zhang Z. Empirical-mechanistic method based stochastic modeling of fatigue damage to predict flexible pavement fatigue cracking for transportation infrastructure management [J]. *Journal of Transportation Engineering*, *ASCE*, 2003, **129**(2): 109-117.
[21] Yoder E J, Witczak M W. *Principles of pavement design* [M]. New York: John Wiley & Sons, Inc, 1975.
[22] Draper N R, Smith H. *Applied regression analysis*[M]. 4th ed. New York: John Wiley & Sons, Inc, 1998.
[23] Johnston J, DiNardo J. *Econometric methods*[M]. 4th ed. McGraw-Hill, 1997.
[24] Wallace S W. Decision making under uncertainty: Is sensitive analysis of any use? [J]. *Operations Research*, 2000, **48**(1): 20-25.
[25] Lehmer D H. Mathematical methods in large-scale computing units[J]. *Annals of the Computation Laboratory of Harvard University*, 1951, **26**: 141-146.
[26] Law A M, Kelton W D. *Simulation modeling and analysis*[M]. 3rd ed. McGraw-Hill, Inc. 2000.
[27] Marsaglia G, Bray T A. A convenient method for generating normal variables[J]. *SIAM Review*, 1964, **6**: 260-264.

路面性能预测中不确定性的量化

孙 璐[1,2] 葛敏莉[1] 顾文钧[1] 徐 冰[1]

([1] 东南大学交通学院,南京 210096)
([2]Department of Civil Engineering, Catholic University of America, Washington DC 20064, USA)

摘要:考虑到路面性能预测中存在的大量可变性和不确定性,为使得路面性能 PSI 的预测结果可信且有意义,提出了一种基于分布的路面性能指标 PSI 预测方法. 该方法建立在 AASHTO 路面性能预测模型基础上,把预测变量处理成具有某种概率分布的随机变量,通过蒙特卡洛数值模拟获得 PSI 的概率分布. 基于路面结构和交通参数建立仿真模型,应用 PERFORM 程序得到数值计算结果. 研究结果表明:交通荷载、表面层材料特性和路面初始性能是影响未来路面性能的最主要因素. 在获得路面性能 PSI 指标的概率分布后,其他统计量如未来路面性能的均值函数和方差函数可以很容易得到.

关键词:路面性能;不确定性;预测; 蒙特卡洛数值模拟
中图分类号:U418.6